Enhancing CRISPR deletion via pharmacological delay of DNA-PK

Núria Bosch (1,2,4),

Michaela Medová (2,3),

Roberta Esposito (1,2),

Carlos Pulido-Quetglas (1,2,4)

Yitzhak Zimmer (2,3),

Rory Johnson* (1,2)

1. Department of Medical Oncology, Inselspital, Bern University Hospital, University of Bern, Switzerland

2. Department for BioMedical Research, University of Bern, Bern, Switzerland

3. Department of Radiation Oncology, Inselspital, Bern University Hospital, University of Bern, Switzerland

4. Graduate School of Cellular and Biomedical Sciences, University of Bern, Bern, Switzerland

*Correspondence: rory.johnson@dbmr.unibe.ch

Keywords: CRISPR; CRISPR deletion ; DNA-PK ; genome editing ; reporter assay; DNA.

Abstract

CRISPR-Cas9 deletion (CRISPR-del) is the leading approach for eliminating DNA from mammalian cells and underpins a variety of genome-editing applications. Target DNA, defined by a pair of double strand breaks (DSBs), is removed during non-homologous end-joining (NHEJ). However, the low efficiency of CRISPR-del results in laborious experiments and false negative results. Using an endogenous reporter system, we demonstrate that temporary inhibition of DNA-dependent protein kinase (DNA-PK) – an early step in NHEJ - yields up to 17-fold increase in DNA deletion. This is observed across diverse cell lines, gene delivery methods, commercial inhibitors and guide RNAs, including those that otherwise display negligible activity. Importantly, the method is compatible with pooled functional screens employing lentivirally-delivered guide RNAs. Thus, delaying the kinetics of NHEJ relative to DSB formation is a simple and effective means of enhancing CRISPR-deletion.

Introduction

CRISPR-Cas9 technology enables a variety of loss-of-function perturbations to study the functions of genomic elements in their natural context, and engineer natural and unnatural mutations[1–3]. One such application, CRISPR-deletion (CRISPR-del), is a means of permanently removing specific genomic fragments from 10^1 – 10^6 base pairs[4]. This range has enabled researchers to investigate a wide variety of functional elements, including gene regulatory sequences[5–7], non-coding RNAs[8–12], and structural elements[13]. Similarly, engineered deletions can be used to model human mutations[14,15]. CRISPR-del is readily scaled to high throughput screens, via pooled lentiviral libraries of thousands of paired single guide RNAs (sgRNAs)[16,17]. This has been used to discover long noncoding RNAs (lncRNAs) regulating cancer cell proliferation[18,19] and to map *cis*-regulatory regions of key protein-coding genes[20,21].

CRISPR-del employs a pair of CRISPR-Cas9 complexes to introduce double strand breaks (DSBs) at two sites flanking the target region. Thereafter it relies on the endogenous non-homologous end joining (NHEJ) process to repair the breaks so as to eject the intervening fragment[22–25]. The two ends of target regions are defined by a pair of user-designed sgRNAs[26]. Paired sgRNAs may be delivered by transfection or viral transduction[17,25]. Pooled screens require that both sgRNAs are encoded in a single vector to ensure their simultaneous delivery, and are typically performed under conditions of low multiplicity-of-infection (MOI), where each cell carries a single lentiviral insertion[18,20,25,27,28].

The principal drawback of CRISPR-del is the low efficiency with which targeted alleles are deleted. Studies on cultured cells typically report efficiencies in the range 0% – 50% of alleles, and often <20%[29,30], similar to estimates from individual clones[4,17,24–26]. Indeed, a recent publication reported high variation in the efficiencies of paired sgRNA targeting the same region, including many that yielded negligible deletion[30]. Transfection typically yields greater efficiency than viral transduction, possibly due to higher sgRNA levels[32], but is incompatible with pooled screening. Although megabase-scale deletions have been reported[33,34], deletion efficiency decreases with increasing target size[4]. Homozygous knockout clones may be isolated by screening hundreds of single cells, however this is slow and laborious, and resulting clones may not be representative of the general population[31]. More important than these practical costs, is the potential impact of low deletion rates on the ability to discern *bona fide* functional effects arising from a given mutation[30]. Non-performing sgRNA

pairs are a particular problem for pooled CRISPR-del screens, where they reduce statistical power and lead to false negative results. To combat this, researchers are forced to increase the coverage of deletion constructs per target, resulting in lower candidate numbers and increased costs[35,36]. Consequently, any method to improve CRISPR-del efficiency would streamline experiments and enable the discovery of presently-overlooked functional elements.

For other applications of CRISPR, most notably precise genome editing using homologous recombination (HR), substantial gains have been made editing efficiency[37]. Here, editing events are rare, and HR is the rate-limiting-step[38,39]. The two principal strategies to boost efficiency are: (1) direct stimulation of homology directed repair (HDR)[37,40–42]; (2) suppression of the competing NHEJ pathway at early stages through inhibition of Ku70/80 complex[37,40,43] or DNA-dependent protein kinase (DNA-PK)[37,40,44,45], or at late phases, via Ligase IV (LigIV) inhibition[37,40,46,47]. To date, however, there are no reported methods for pharmacological enhancement of CRISPR-del.

Towards this aim, we consider the events necessary for successful deletion (Fig. 3). In the presence of two DSBs, NHEJ gives rise to successful deletion. For this to occur, the DSBs must occur on a timescale shorter than that required for NHEJ. Otherwise, the first DSB is repaired by NHEJ *before* the second can occur, and deletion will not take place. Furthermore, there is a high probability that the target protospacer or protospacer adjacent motif (PAM) is mutated during NHEJ, rendering it inaccessible to the sgRNA and precluding any subsequent deletion.

A prediction of this model, is that successful deletion can be promoted by extending the time over which DSBs persist without being repaired, and hence increasing the likelihood that both DSBs co-occur. In other words, we hypothesise that CRISPR-del may be improved by pharmacologically slowing the rate of NHEJ during the period while DSBs are taking place. Here, we show that inhibition of DNA-PK, an early step in NHEJ, indeed improves CRISPR-del efficiency, regardless of cell type, target region, sgRNA or inhibitory molecule, and represents a practical strategy for a variety of applications including pooled library screening.

Results

A quantitative endogenous reporter for CRISPR-del

To identify factors capable of improving CRISPR-del efficiency, we designed a gene-based reporter system: CRISPR Deletion Endogenous Reporter (CiDER). Such a system should be quantitative, sensitive, practical and able to closely model the CRISPR-del process by targeting endogenous genes rather than plasmids. We focussed on genes encoding cell-surface proteins, as they can be rapidly and sensitively detected by flow cytometry[48]. A number of candidates were considered with criteria of (1) non-essentiality for cell viability and proliferation[49–51](https://depmap.org), (2) high expression in human cell lines[52] (http://www.proteinatlas.org), (3) lack of overlap with other genomic elements that could lead to false positive detection, and (4) availability of flow-cytometry grade antibody. Consequently, we selected *PLXND1* encoding the Plexin-D1 protein (Supplementary Fig. 1).

We conceived an experimental setup where only successful CRISPR-del leads to loss of *PLXND1* expression, but unsuccessful events do not. In this scheme, the gene's first exon is targeted for deletion by a series of sgRNA pairs recognising the non-protein coding regions upstream (promoter) and downstream (first intron) (Fig. 1a). Successful deletions of the first exon are expected to silence protein expression, but indels from individual sgRNAs do not affect the protein sequence directly and should not lead to silencing. Finally, we also designed sgRNAs that directly target the open reading frame (ORF), since these are expected to yield maximal protein silencing (designated positive control, *P+*).

We used flow cytometry to evaluate Plexin-D1 protein levels (Fig. 1b). Positive control sgRNAs (*P+*) yielded approximately 90% knockout efficiency. We observed wide variability in the deletion efficiency of sgRNA pairs, from Pair1 (*P1*) displaying minimal efficacy, to the most efficient *P4* yielding ~40% deletion. Therefore these paired sgRNAs achieve deletion efficiencies that are comparable to previous studies[4,26]. Measured deletion rates were consistent across biological replicates (Fig. 1b). The observed loss of Plexin-D1 was not due to large indels or disruption of gene regulatory elements at individual sgRNA target sites[53], since control experiments with single sgRNAs showed no loss of Plexin-D1 (Supplementary Fig. 2). In CiDER we have a reproducible and practical reporter of CRISPR-del at a range of efficiencies.

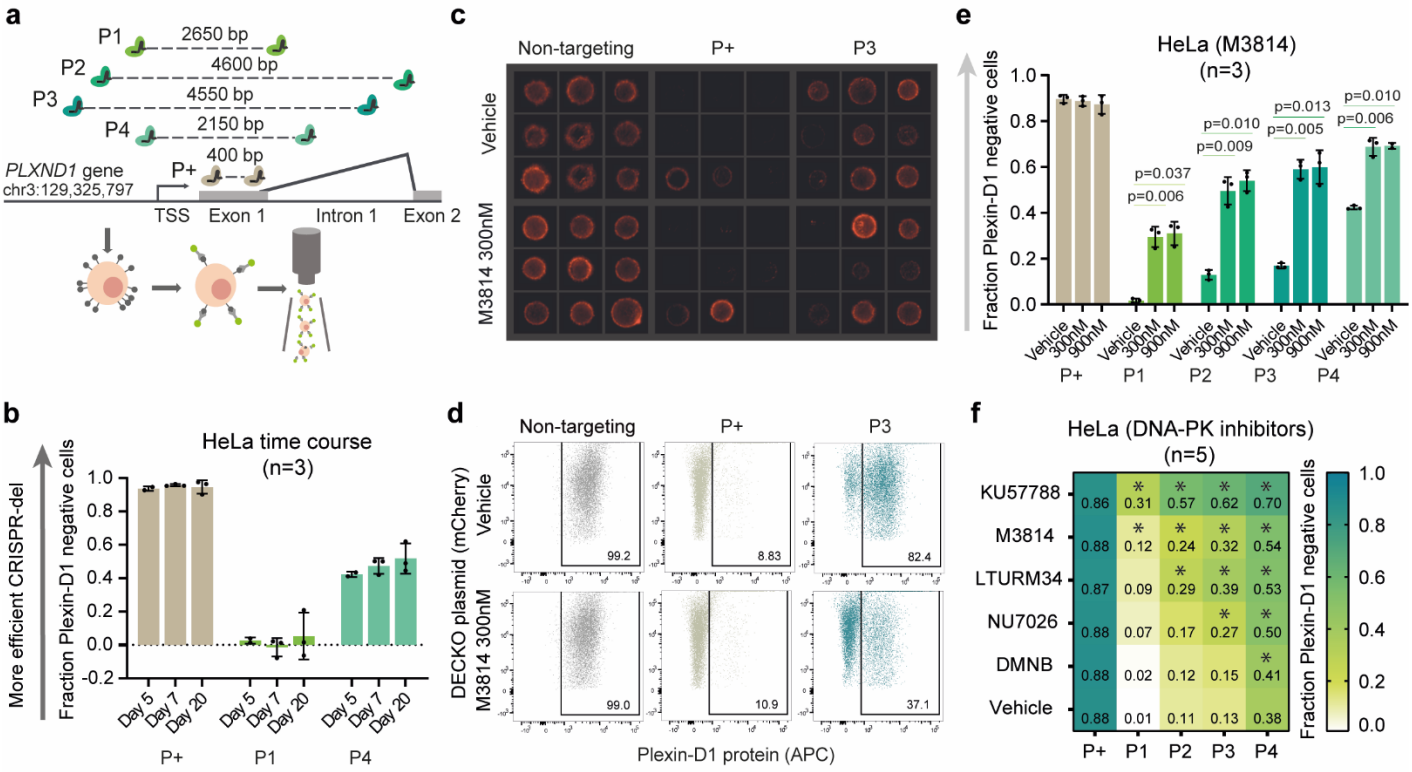

Fig. 1| CiDER reporter system identifies DNA-PK inhibition as a means to increase CRISPR-del efficiency. a, The CiDER endogenous reporter relies on a series of sgRNA pairs targeting exon 1 of *PLXND1* locus, whose protein product is read out by flow cytometry. **b,** CRISPR-del efficiency time course in HeLa (mean, standard deviation). **c,** Representative images of Plexin-D1 (APC) staining in HeLa. **d,** Representative raw flow cytometry plots of CiDER in HeLa upon DNA-PK inhibition. Plexin-D1 positive cells are gated and numbers correspond to percentage of cells. **e,** CRISPR-del efficiency of CiDER in HeLa upon DNA-PK inhibition (mean, standard deviation, 2-tailed paired *t*-test). **f,** CRISPR-del efficiency of CiDER in HeLa upon DNA-PK inhibition with different small molecules (mean and 2-tailed paired *t*-test).

Temporary inhibition of DNA-PK during DSB formation increases CRISPR-del efficiency

We hypothesized that temporarily inhibiting NHEJ during DSB formation would favour CRISPR-del, by increasing the chance that both DSBs will co-occur (Fig. 3). We tested DNA-PK, a DNA end-binding factor at the first step of NHEJ pathway, for which a number of small-molecule inhibitors are available[54]. We began by treating HeLa cells with the inhibitor M3814 (IC_{50}=3nM) [45,55,56] at two concentrations (300 nM and 900 nM). Importantly, cells constitutively expressing Cas9 were treated for an 18 hour time window, 4 hours after sgRNA expression plasmid delivery by transfection. Thus, DNA-PK was inhibited immediately before sgRNA expression. This resulted in improved deletion rates for all four sgRNA pairs, including a 17-fold increase for *P1*, which otherwise displays negligible deletion under normal conditions (Fig. 1c,e).

We next asked whether other inhibitors of DNA-PK yield a similar effect. We treated cells with four other commercially-available molecules at a concentration of 10uM: KU57788 (IC_{50}=14nM), NU7026 (IC_{50}=230nM), LTURM34 (IC_{50}=34nM) and DMNB (IC_{50}=15uM) (Fig. 1f). Each one yielded increases in CRISPR-del efficiency to varying degrees, correlating with published differences on the inhibition potency[57]. As expected based on previous literature, KU57788 gave the strongest effect[57] and DMNB gave the weakest effect, likely due to its high IC_{50}.

We were curious whether improved deletion depends on inhibition specifically of DNA-PK, or more generally on NHEJ. To answer this, we used SCR7 pyrazine to inhibit another step in NHEJ, the final ligation by Ligase IV (LigIV). In contrast to DNA-PK, this treatment did not improve deletion efficiency (Fig. 2a). At this late stage, the NHEJ machinery (DNA-end binding and processing complex) is already maintaining together the free DNA ends. When LigIV activity is restored, it may be more likely that each single DSB is repaired independently, introducing small indels rather than favouring genomic deletion. Thus, CRISPR-del efficiency improvements depend specifically on inhibition of DNA-PK activity. Altogether, we have shown that pharmacological inhibition of NHEJ at the DNA-PK step yields enhanced deletion of *PLXND1* reporter in HeLa cells.

Generality of deletion enhancement by DNA-PK inhibition

We next assessed whether this DNA-PK-inhibition is more generally effective across cell lines, genomic targets and sgRNA delivery modalities.

We began by replicating CiDER experiments in two widely-used cell lines, HCT116 and HEK293T[30,58–60] (Fig. 2b). Both have baseline CRISPR-del efficiency below HeLa, possibly due to weaker NHEJ activity[39]. Nevertheless, DNA-PK inhibition enhanced deletion in both cell backgrounds.

All experiments so far involved a single target locus, assayed by flow cytometry. We next assessed whether these effects hold for other loci and readouts. We previously used a quantitative PCR method (quantitative CRISPR PCR, QC-PCR) to measure rates of deletion at the *MALAT1* enhancer region[26]. For three out of four sgRNA pairs, we observed a significant enhancement of deletion with M3814 treatment of HeLa (Fig. 2c, note

the inverted scale used for QC-PCR). Similar but weaker results were also observed for HCT116 (two out of four pairs) and HEK293T cells (one out of four pairs) (Supplementary Fig. 3).

Together, these findings support the general applicability of DNA-PK inhibition independent of cell line or target regions.

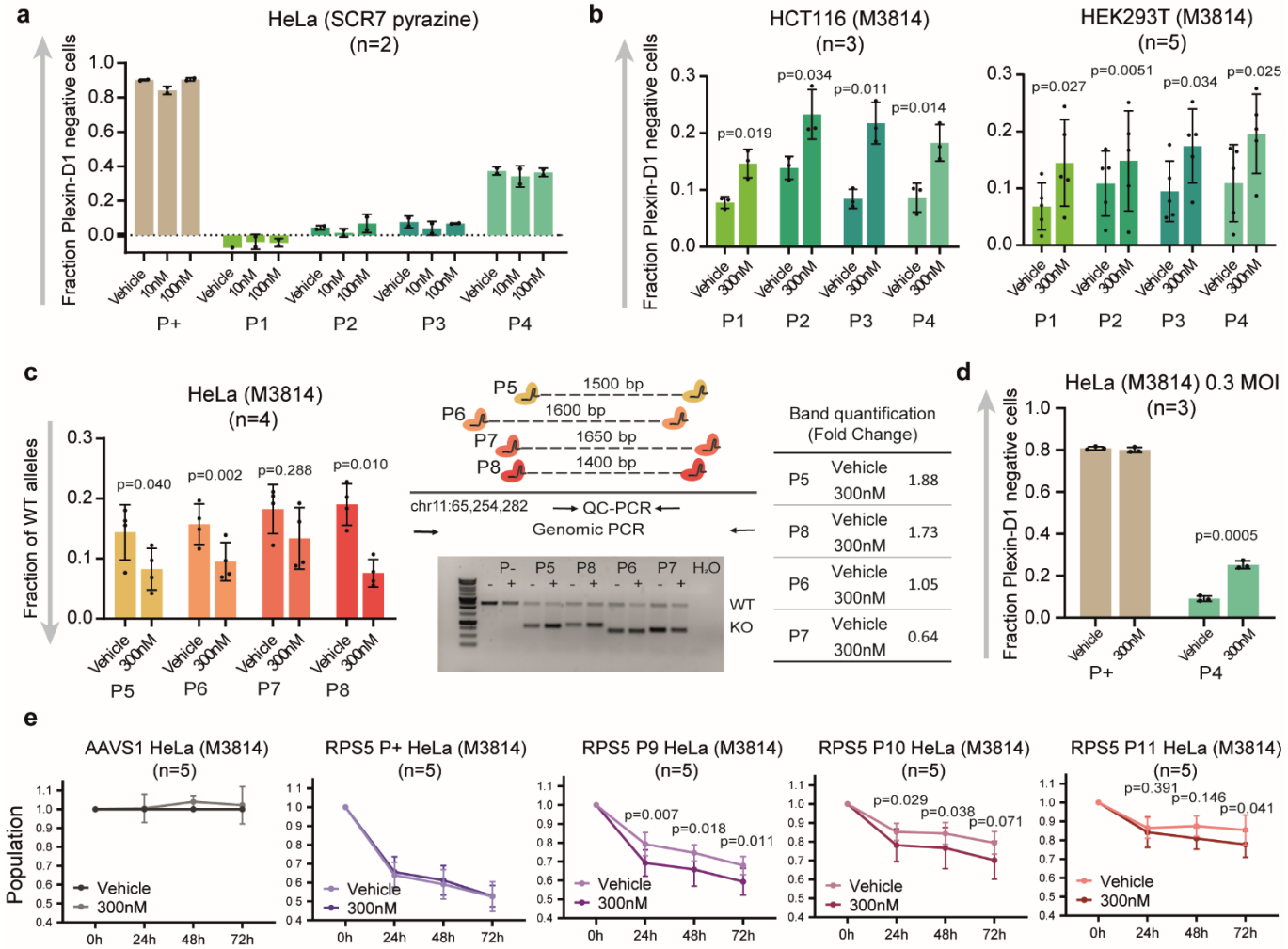

Fig. 2| Universality of DNA-PK inhibition. a, CRISPR-del efficiency of CiDER in HCT116 and HEK293T cell lines upon DNA-PK inhibition (mean, standard deviation, 2-tailed paired *t*-test). **b,** CRISPR-del efficiency in chr11-locus in HeLa upon DNA-PK inhibition. The bar plots show the fraction of WT allele quantified by qPCR (mean, standard deviation, 2-tailed paired *t*-test). Shown a scheme of the sgRNA pairs and PCR primers design for this locus. Also shown a representative agarose gel from the genomic PCR of the region and band quantification of the KO allele. **c,** CRISPR-del efficiency of CiDER in HeLa upon LigIV inhibition (mean, standard deviation). **d,** CRISPR-del efficiency of CiDER in HeLa upon low MOI lentiviral infection and DNA-PK inhibition (mean, standard deviation, 2-tailed paired *t*-test). **e,** Functional validation of DNA-PK inhibition. Viability assays after RPS5 TSS deletion upon DNA-PK inhibition (mean, standard deviation, 2-tailed paired *t*-test).

DNA-PK inhibition in the context of high-throughput pooled screens

CRISPR-del perturbations can be employed in the context of pooled functional screens, where libraries of paired sgRNAs are delivered by lentivirus at low MOI, and the effect on phenotypes such as proliferation are recorded. We asked whether DNA-PK inhibition is also practical under these conditions, by targeting the *PLXND1* reporter with sgRNAs delivered by low-MOI lentivirus. In initial experiments, M3814 was added to cell media prior to lentiviral transduction, but no improvement in deletion efficiency was observed (data not shown). This is explained by the fact that lentiviruses require NHEJ for genomic integration[61,62]. Therefore, we modified our protocol so as to leave sufficient time for viral integration before NHEJ inhibition (24 h was optimal, Supplementary Fig. 4), and observed a 2.7-fold increase in CRISPR-del efficiency (Fig. 2d).

Pooled CRISPR screens employ phenotypic readouts, often in the form of cell proliferation[3,27]. To test whether improved CRISPR-del translates into stronger phenotypes, we developed a reporter assay capable of quantifying the phenotypic effect of CRISPR-del in terms of cell death. Analagous to *PLXND1* (Fig. 1a), We designed three pairs of sgRNAs targeting the first exon of the essential gene, *RPS5* (coding for the 40S ribosomal protein S5, P46782, Uniprot): *RPS5-P+*, *P9*, *P10*, *P11*. As expected, sgRNAs targeting the *AAVS1* locus had no effect, while sgRNAs targeting the RPS5 ORF (*RPS5-P+*) resulted in ~47% mortality after 72 h (Fig. 2e). Neither was affected by M3814, indicating no toxicity. In contrast, three pairs of sgRNAs targeting the first exon of *RPS5* (*P9*, *P10*, *P11*) resulted in a substantial mortality (32%, 21% and 15%, respectively), which was significantly enhanced by addition of M3814 (41%, 30% and 22%, respectively).

In conclusion, DNA-PK inhibition enhances CRISPR-del when sgRNAs are delivered lentivirally at low MOI, and results in increased downstream phenotypic effects, supporting its utility in the context of high-throughput pooled screens.

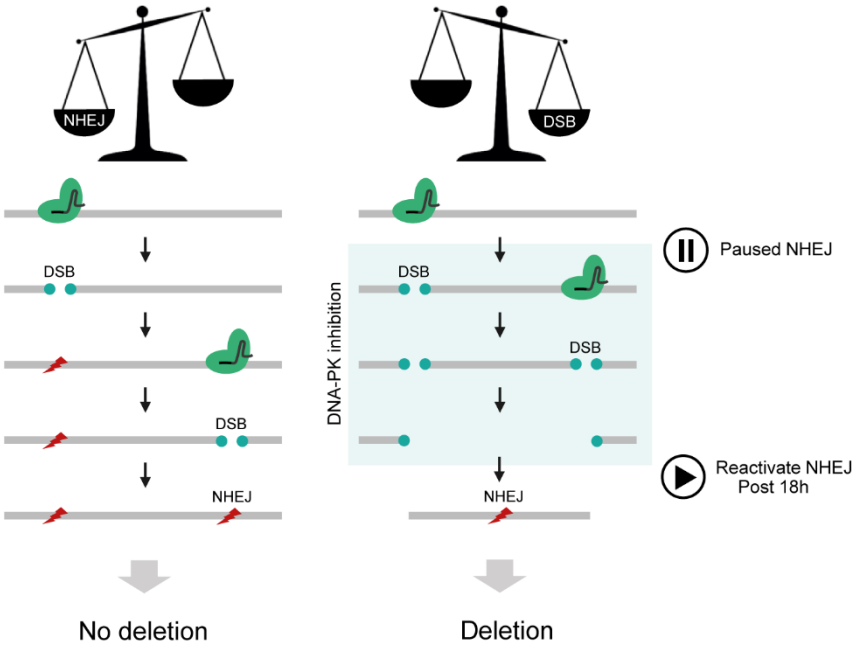

Fig. 3| Model for CRISPR-deletion and its improvement by inhibition of DNA-PK.

Discussion

The intrinsic DNA damage response underpins CRISPR-Cas9 genome editing and may be manipulated to favour desired editing outcomes. In the case of precise genome editing, which is based on the HDR pathway, efficiency has been substantially improved through pharmacological promotion of HDR and inhibition of the competing NHEJ pathway[37]. No such solutions have been developed for CRISPR-del, despite its being one of the most common CRISPR-Cas9 modalities, with diverse scientific and technological applications[5–15].

We hypothesised that successful CRISPR-del requires paired DSBs to co-occur *before* NHEJ has time to act, and thus may be enhanced by pharmacological inhibition of DNA-PK. This is initially counter-intuitive, as DNA-PK is a necessary step in the NHEJ pathway upon which CRISPR-del relies, and its inhibition is widely used to promote HDR[37,40,44,45]. However, rather than permanently blocking NHEJ, our protocol slows the kinetics of NHEJ for a defined period while DSBs are taking place. This produces a significant enhancement of DNA deletion efficiency, increasing protein knockout rates and resulting in stronger functional effects.

DNA-PK inhibition represents a practical option for a variety of CRISPR-del applications, from basic research to gene therapy. DNA-PK inhibitors are cheap and widely-available. Deletion efficiency improved regardless of the inhibitor molecule, target region, sgRNA sequence, cell background and delivery method. Particularly striking was the observation that some sgRNA pairs that are ineffective under normal conditions, achieved respectable rates of deletion using DNA-PK inhibition. This suggests that the failure of many sgRNA pairs to efficiently delete DNA arises not from their inability to promote DSBs, but rather as a result of poor kinetic properties (for example, a mismatch in kinetics between the two individual sgRNAs). Finally, this method (with minor modifications) is compatible with low-MOI lentiviral delivery and leads to improvements in observed cell phenotypes. These conditions are employed in pooled screens to probe the functions of non-protein coding genomic elements[18–21], meaning that DNA-PK inhibition may be used in future to improve the sensitivity of CRISPR-deletion screens by boosting the number of active sgRNA pairs, and their efficiency.

References

1. Cong, L. *et al.* Multiplex Genome Engineering Using CRISPR/Cas Systems. *Science (80-.).* 819–823 (2013). doi:10.1126/science.1231143
2. Mali, P. *et al.* RNA-Guided Human Genome Engineering via Cas9. *Science* **339**, 823–827 (2013).
3. Doench, J. G. Am I ready for CRISPR? A user's guide to genetic screens. *Nat. Rev. Genet.* **19**, 67–80 (2017).
4. Canver, M. C. *et al.* Characterization of genomic deletion efficiency mediated by CRISPR/Cas9 in mammalian cells. *J. Biol. Chem.* **289**, 21312–21324 (2014).
5. Canver, M. C. *et al.* BCL11A enhancer dissection by Cas9- mediated in situ saturating mutagenesis. *Nature* **527**, (2015).
6. Mochizuki, Y. *et al.* Combinatorial CRISPR/Cas9 Approach to Elucidate a Far-Upstream Enhancer Complex for Tissue- Specific Sox9 Expression. *Dev. Cell* **46**, 794-806.e6 (2018).
7. Gasperini, M. *et al.* A Genome-wide Framework for Mapping Gene Regulation via Cellular Genetic Screens. *Cell* **176**, 377–390 (2019).
8. Han, J. *et al.* Efficient in vivo deletion of a large imprinted lncRNA by CRISPR/Cas9. *RNA Biol.* **11**, 829–35 (2014).
9. Ho, T.-T. *et al.* Targeting non-coding RNAs with the CRISPR/Cas9 system in human cell lines. *Nucleic Acids Res.* **43**, e17 (2015).
10. Holdt, L. M. *et al.* Circular non-coding RNA ANRIL modulates ribosomal RNA maturation and atherosclerosis in humans. *Nat. Commun.* **7**, (2016).
11. Koirala, P. *et al.* LncRNA AK023948 is a positive regulator of AKT. *Nat. Commun.* **8**, 14422 (2017).
12. Xing, Y.-H. *et al.* SLERT Regulates DDX21 Rings Associated with Pol I Transcription. *Cell* **169**, 664-670.e16 (2017).
13. Huang, J. *et al.* Dissecting super-enhancer hierarchy based on chromatin interactions. *Nat. Commun.* **9**, (2018).

14. Lupiañez, D. G. *et al.* Disruptions of Topological Chromatin Domains Cause Pathogenic Rewiring of Gene-Enhancer Interactions. *Cell* **161**, 1012–1025 (2015).

15. Nelson, C. E. *et al.* In vivo genome editing improves muscle function in a mouse model of Duchenne muscular dystrophy. **351**, 403–408 (2016).

16. Vidigal, J. A. & Ventura, A. Rapid and efficient one-step generation of paired gRNA CRISPR-Cas9 libraries. *Nat. Commun.* **6**, 8083 (2015).

17. Aparicio-Prat, E. *et al.* DECKO: Single-oligo, dual-CRISPR deletion of genomic elements including long non-coding RNAs. *BMC Genomics* **16**, 846 (2015).

18. Zhu, S. *et al.* Genome-scale deletion screening of human long non-coding rNAs using a paired-guide rNA crisPr–cas9 library. *Nat. Biotechnol.* **34**, (2016).

19. Liu, Y. *et al.* Genome-wide screening for functional long noncoding RNAs in human cells by Cas9 targeting of splice sites. *Nat. Biotechnol.* **36**, (2018).

20. Gasperini, M. *et al.* CRISPR/Cas9-Mediated Scanning for Regulatory Elements Required for HPRT1 Expression via Thousands of Large, Programmed Genomic Deletions. *Am. J. Hum. Genet.* (2017).

21. Diao, Y. *et al.* A tiling-deletion-based genetic screen for cis - regulatory element identification in mammalian cells. *Nat. Methods* **14**, (2017).

22. Yang, H. *et al.* One-Step Generation of Mice Carrying Reporter and Conditional Alleles by CRISPR/Cas-MediatedGenome Engineering. *Cell* **154**, 1370–1379 (2013).

23. Maddalo, D. *et al.* In vivo engineering of oncogenic chromosomal rearrangements with the CRISPR/Cas9 system Danilo. *Nature* **516**, (2014).

24. Ho, T.-T. *et al.* Targeting non-coding RNAs with the CRISPR/Cas9 system in human cell lines. *Nucleic Acids Res.* **43**, e17 (2015).

25. Vidigal, J. A. & Ventura, A. Rapid and efficient one-step generation of paired gRNA CRISPR-Cas9 libraries. *Nat. Commun.* **6**, 1–7 (2015).

26. Pulido-Quetglas, C. *et al.* Scalable Design of Paired CRISPR Guide RNAs for Genomic Deletion. *PLOS Comput. Biol.* **13**, e1005341 (2017).

27. Esposito, R. *et al.* Hacking the Cancer Genome: Profiling Therapeutically Actionable Long Non-

coding RNAs Using CRISPR-Cas9 Screening. *Cancer Cell* **35**, 545–557 (2019).

28. Doench, J. G. Am I ready for CRISPR? A user's guide to genetic screens. *Nat. Rev. Genet.* **19**, 67–80 (2018).
29. Mandal, P. K. *et al.* Efficient Ablation of Genes in Human Hematopoietic Stem and Effector Cells using CRISPR/Cas9. *Cell Stem Cell* **15**, 643–652 (2014).
30. Thomas, J. D. *et al.* RNA isoform screens uncover the essentiality and tumor-suppressor activity of ultraconserved poison exons. *Nat. Genet.* **52**, (2020).
31. Stojic, L. *et al.* Specificity of RNAi, LNA and CRISPRi as loss-of-function methods in transcriptional analysis. *Nucleic Acids Res.* **46**, 5950–5966 (2018).
32. Mangeot, P. E. *et al.* Genome editing in primary cells and in vivo using viral-derived Nanoblades loaded with Cas9-sgRNA ribonucleoproteins. *Nat. Commun.* **10**, 1–15 (2019).
33. Han, J. *et al.* Efficient in vivo deletion of a large imprinted lncRNA by CRISPR/Cas9. *RNA Biol.* **11**, 829–835 (2014).
34. Essletzbichler, P. *et al.* Megabase-scale deletion using CRISPR / Cas9 to generate a fully haploid human cell line. *Genome Res.* **24**, 2059–2065 (2014).
35. Doench, J. G. *et al.* Optimized sgRNA design to maximize activity and minimize off-target effects of CRISPR-Cas9. *Nat. Biotechnol.* **34**, 184–191 (2016).
36. Sanson, K. R. *et al.* Optimized libraries for CRISPR-Cas9 genetic screens with multiple modalities. *Nat. Commun.* **9**, 5416 (2018).
37. Yeh, C. D., Richardson, C. D. & Corn, J. E. Advances in genome editing through control of DNA repair pathways. *Nat. Cell Biol.* **21**, (2019).
38. Mao, Z., Bozzella, M., Seluanov, A. & Gorbunova, V. Comparison of nonhomologous end joining and homologous recombination in human cells. *DNA Repair (Amst).* **7**, 1765–1771 (2008).
39. Miyaoka, Y. *et al.* Systematic quantification of HDR and NHEJ reveals effects of locus, nuclease, and cell type on genome- editing. *Sci. Rep.* 1–12 (2016). doi:10.1038/srep23549
40. Riesenberg, S. & Maricic, T. Targeting repair pathways with small molecules increases precise genome editing in pluripotent stem cells. *Nat. Commun.* **9**, 1–9 (2018).

41. Song, J. *et al.* RS-1 enhances CRISPR/Cas9- and TALEN-mediated knock-in efficiency. *Nat. Commun.* **7**, (2016).

42. Lin, S., Staahl, B. T., Alla, R. K. & Doudna, J. A. Enhanced homology-directed human genome engineering by controlled timing of CRISPR / Cas9 delivery. *Elife* 1–13 (2014). doi:10.7554/eLife.04766

43. Fattah, F. J., Lichter, N. F., Fattah, K. R., Oh, S. & Hendrickson, E. A. Ku70 , an essential gene , modulates the frequency of rAAV-mediated gene targeting in human somatic cells. *PNAS* **105**, 8703–8708 (2008).

44. Robert, F., Barbeau, M., Éthier, S., Dostie, J. & Pelletier, J. Pharmacological inhibition of DNA-PK stimulates Cas9-mediated genome editing. *Genome Med.* 1–11 (2015). doi:10.1186/s13073-015-0215-6

45. Riesenberg, S., Chintalapati, M., Macak, D. & Kanis, P. Simultaneous precise editing of multiple genes in human cells. *Nucleic Acids Res.* **47**, (2019).

46. Chu, V. T. *et al.* Increasing the efficiency of homology-directed repair for CrIsPr-Cas9-induced precise gene editing in mammalian cells. *Nat. Biotechnol.* **33**, (2015).

47. Maruyama, T. *et al.* Increasing the efficiency of precise genome editing with CrIsPr-Cas9 by inhibition of nonhomologous end joining. *Nat. Biotechnol.* **33**, 1–9 (2015).

48. Bausch-Fluck, D. *et al.* A Mass Spectrometric-Derived Cell Surface Protein Atlas. *PLoS One* 1–22 (2015). doi:10.1371/journal.pone.0121314

49. Luo, B. *et al.* Highly parallel identification of essential genes in cancer cells. *PNAS* **105**, 20380–5 (2008).

50. Meyers, R. M. *et al.* Computational correction of copy number effect improves specificity of CRISPR-Cas9 essentiality screens in cancer cells. *Nat. Genet.* **49**, 1779–1784 (2017).

51. Tsherniak, A. *et al.* Defining a Cancer Dependency Map. *Cell* **170**, 564-576.e16 (2017).

52. Thul, P. J. *et al.* A subcellular map of the human proteome. *Science (80-.).* **356**, eaal3321 (2017).

53. Kosicki, M., Tomberg, K. & Bradley, A. Repair of double-strand breaks induced by CRISPR – Cas9 leads to large deletions and complex rearrangements. *Nat. Biotechnol.* **36**, (2018).

54. Harnor, S. J., Brennan, A. & Cano, C. Targeting DNA-Dependent Protein Kinase for Cancer Therapy. *ChemMedChem* **12**, 895–900 (2017).

55. Fuchss, T., Emde, U., Buchstaller, H.-P. & W.K.R., W. M. WO2014183850A1. (2014).

56. Zenke, F. T. *et al.* Abstract 1658: M3814, a novel investigational DNA-PK inhibitor: enhancing the effect of fractionated radiotherapy leading to complete regression of tumors in mice. in *Proceedingsof the 108thAnnual Meeting of theAmericanAssociation for CancerResearch* (2016).

57. Mohiuddin, I. S. & Kang, M. H. DNA-PK as an Emerging Therapeutic Target in Cancer. **9**, 1–8 (2019).

58. Li, N. & Richard, S. Sam68 functions as a transcriptional coactivator of the p53 tumor suppressor. *Nucleic Acids Res.* 1–16 (2016). doi:10.1093/nar/gkw582

59. Hart, T. *et al.* High-Resolution CRISPR Screens Reveal Fitness Genes and Genotype-Specific Cancer Liabilities. (2015). doi:10.1016/j.cell.2015.11.015

60. Liu, S. J. *et al.* CRISPRi-based genome-scale identification of functional long noncoding RNA loci in human cells. *Science (80-.).* **355**, eaah7111 (2017).

61. Li, L. *et al.* Role of the non-homologous DNA end joining pathway in the early steps of retroviral infection. *EMBO J* **20**, (2001).

62. Rene, D. *et al.* Evidence that Stable Retroviral Transduction and Cell Survival following DNA Integration Depend on Components of the Nonhomologous End Joining Repair Pathway. *J. Virol.* **78**, 8573–8581 (2004).

63. Schmittgen, T. D. & Livak, K. J. Analyzing real-time PCR data by the comparative CT method. *Nat. Protoc.* **3**, 1101–1108 (2008).

Acknowledgements

We gratefully acknowledge administrative support from Ana Radovanovic and Silvia Roesselet (DBMR, University of Bern). We thank Bill Keyes (IGBMC) and Norbert Polacek (DCB, University of Bern) for insightful feedback and discussions. We also thank Stefan Müller (DBMR, University of Bern) for his expertise with ImageStream and the other members of the FACS lab from the University of Bern for their advice. We also acknowledge Taisia Polidori and Paulina Schaerer (DBMR, University of Bern) for the experimental support and the rest of the members of Johnson's lab for their valuable input. Andrea Maddalena (Department of Physiology, University of Bern) provided valuable advice regarding lentiviral transduction inhibition. This work was funded by the Swiss National Science Foundation through the National Center of Competence in Research (NCCR) "RNA & Disease", by the Medical Faculty of the University and University Hospital of Bern, by the Helmut Horten Stiftung and Krebsliga Schweiz (4534-08-2018).

Author contributions

N.B. and R.J. conceived and designed the experiments. N.B. performed all the experiments. M.M. and Y.Z. suggested DNA-PK inhibition to modulate NHEJ. C.P. contributed on the design of the sgRNA pairs. R.E. provided the solution to circumvent lentiviral infection problems. N.B. and R.J. wrote the whole manuscript with feedback from M.M. and Y.Z. Finally, R.J. directed the research.

Competing interests

The authors declare that they do not have competing interests.

Materials and methods

Cell culture. HeLa, HCT116 and HEK293T were cultured on Dulbecco's Modified Eagles Medium (DMEM) (Sigma-Aldrich, D5671) supplemented with 10% Fetal Bovine Serum (FBS) (ThermoFisher Scientific, 10500064), 1% L-Glutamine (ThermoFisher Scientific, 25030024), 1% Penicillin-Streptomycin (ThermoFisher Scientific, 15140122). Cells were grown at 37°C and 5% CO_2 and passaged every two days at 1:5 dilution.

Generation of Cas9 stable cell lines. HeLa cells were infected with lentivirus carrying the Cas9-BFP (blue fluorescent protein) vector (Addgene 52962). HCT116 and HEK293T were transfected with the same vector using Lipofectamine 2000 (ThermoFisher Scientific, 11668019). All cell types were selected with blasticidin (4ug/ml) for at least five days and selected for BFP-positive cells twice by fluorescence activated cell sorting.

sgRNA pair design and cloning. sgRNA pairs were designed using CRISPETa (http://crispeta.crg.eu/) and cloned into the pDECKO backbone as described previously[26]. Off-target filters did not allow less than 3 mismatches for each sgRNA sequence. No positive or negative masks were applied in the search. Minimum individual score was set at 0.2 and minimum paired score at 0.4. The sgRNA pairs were then manually selected from the output list. All sgRNA sequences may be found in Supplementary Figure 5.

Inhibitors. All molecules used in this study are commercially available: M3814 (MedChemExpress, HY-101570), KU57788 (MedChemExpress, HY-11006), NU7026 (MedChemExpress, HY-15719), LTURM34 (MedChemExpress, HY-101667), DMNB (ToChris, 2088) and SCR7 Pyrazine (Sigma-Aldrich, SML1546). 10mM stocks (and 5mM for NU7026, due to solubility limitations) were prepared by resuspension in dimethylsulfoxide (DMSO) (Sigma-Aldrich, D4540).

Transfection and lentiviral transduction. For transfection experiments, 70% confluent 12-well plates were transfected using Lipofectamine 2000 (ThermoFisher Scientific, 11668019) with 1250 ng of pDECKO plasmid following provider's guidelines. After 6 hours, transfection media was replaced for fresh complete DMEM (10% FBS, 1% L-Glutamine and 1% Penicillin-Streptomycin) and the corresponding small molecule was added to

media for 18 hours. The treatment was finished by replacing the media with complete DMEM. After one day cells were selected with puromycin (2ug/ml).

For lentiviral infection experiments, cells were spin-infected at a 0.3 multiplicity of infection in the presence of DMEM (10% FBS, 1% L-Glutamine) and hexadimethrine bromide (8ug/ml) (Sigma-Aldrich, 107689) at 2000 rpm, 37°C during 1.5 hours. After 0, 5, 10, 24, 48, 72 hours, infection media was replaced for fresh complete DMEM (10% FBS, 1% L-Glutamine and 1% Penicillin-Streptomycin) and the corresponding small molecule was added to media for 18 hours. The treatment was finished by replacing the media with complete DMEM and puromycin (2ug/ml) to start the selection.

Flow cytometry. After five days of puromycin selection, cells were trypsinized, resuspended in PBS and incubated for 30 minutes at room temperature (RT) with the human α-PlexinD1 mouse monoclonal antibody (1:150 dilution) (R&D systems, MAB4160). Cells were washed twice with PBS and incubated for 30 minutes at RT with an α-Mouse IgG secondary goat antibody conjugated to the APC fluorochrome (1:200 dilution) (eBioscience, 17-4010-82). Cells were washed and resuspended in PBS, processed with the LSRII SORP flow cytometer and analysed with FlowJo_v10 software. A total of 10,000 cells per sample are sorted. Cell population is selected in the SSC-A/FSC-A plot. Single cells are gated in the FSC-H/FSC-A plot. Finally, the APC positive population is set in the mCherry/APC plot in the control sample and expanded to all the other samples without modification. The fraction of Plexin-D1 negative singlet cells is calculated by gating Plexin-D1 positive singlet cells, normalizing to a non-targeting control and subtracting the value to 1 (negative cells = 1 – positive cells). An example of the gating strategy may be found in Supplementary Figure 6.

Single cell imaging was performed using ImageStream (Luminex) and analysed with IDEAS software.

Genomic PCRs. After 5 days of puromycin selection, cells were collected and genomic DNA (qDNA) was extracted using GeneJET Genomic DNA Purification Kit (ThermoFisher Scientific, K0722). Genomic PCR was performed using GoTaq® G2 DNA Polymerase (Promega, M7841) from 10ng gDNA (Forward: *5' CCTGCTATGAACTGACCCATG 3'*, Reverse: *5' CCTGAACAGTCAGTCCATGCT 3'*)

Genomic quantitative PCRs. After 5 days of puromycin selection, cells were collected and genomic DNA (qDNA) was extracted using GeneJET Genomic DNA Purification Kit (ThermoFisher Scientific, K0722). Quantitative real time PCR (qPCR) from 10ng of gDNA was performed using GoTaq qPCR Master Mix (Promega, A6001) on a TaqMan Viia 7 Real-Time PCR System. (Target sequence - Forward: *5' GCTGGGGAATCCACAGAGAC 3'*, Reverse: *5' CATCTCAGCCCTTGTTATCCTG 3'*) and (LDHA - Forward: *5' TGGGCAGTAGAAAGTGCAG 3'*, Reverse: *5' TACCAGCTCCCACTCACAG 3'*). Target sequence primers were normalized to primers targeting the distal, non-targeted gene LDHA. Data were normalised using the ΔΔCt method[63].

Cell viability assay. CellTiter-Glo® 2.0 Cell Viability Assay (Promega, G9241) was performed upon puromycin selection (2 days post transfection). 3000 cells/well were seeded in 96-well white polystyrene plates (Corning®, Sigma-Aldrich CLS3610-48EA) and cell viability was measured in technical duplicates during 4 consecutive days (0h, 24h, 48h, 72h) according to the manufacturer's protocol. Luminescence was measured using a Tecan Reader Infinite 200.

Reporting summary. Further information is available in the Nature Research Reporting Summary linked to this article.

Data availability

The authors declare that all the data supporting the findings of this study are available within the paper and its supplementary information files.